A role for α- and β-catenins in bacterial uptake

Marc Lecuit*, Reini Hurme*, Javier Pizarro-Cerdá*, Hélène Ohayon†, Benjamin Geiger‡, and Pascale Cossart*§

*Unité des Interactions Bactéries-Cellules, †Station Centrale de Microscopie Electronique, Institut Pasteur, 28 rue du Docteur Roux, 75724 Paris Cedex 15, France; and ‡Department of Molecular Cell Biology, Weizmann Institute, 76100 Rehovot, Israel

Communicated by Elaine Fuchs, The University of Chicago, Chicago, IL, June 30, 2000 (received for review May 11, 2000)

Interaction of internalin with E-cadherin promotes entry of *Listeria monocytogenes* into human epithelial cells. This process requires actin cytoskeleton rearrangements. Here we show, by using a series of stably transfected cell lines expressing E-cadherin variants, that the ectodomain of E-cadherin is sufficient for bacterial adherence and that the intracytoplasmic domain is required for entry. The critical cytoplasmic region was further mapped to the β-catenin binding domain. Because β-catenin is known to interact with α-catenin, which binds to actin, we generated a fusion molecule consisting of the ectodomain of E-cadherin and the actin binding site of α-catenin. Cells expressing this chimera were as permissive as E-cadherin-expressing cells. In agreement with these data, α- and β-catenins as well as E-cadherin clustered and colocalized at the entry site, where F-actin then accumulated. Taken together, these results reveal that E-cadherin, via β- and α-catenins, can trigger dynamic events of actin polymerization and membrane extensions culminating in bacterial uptake.

Listeria monocytogenes is a human foodborne pathogen causing meningitis, encephalitis, and mother-to-child infections (1). *L. monocytogenes* crosses three barriers during the infectious process: the intestinal barrier, the blood-brain barrier, and the fœtoplacental barrier. The molecular basis of these key events are unknown, in contrast to those allowing *L. monocytogenes* entry into tissue culture cells, which have been studied in detail (2). Entry is mediated by two leucine-rich repeat bacterial proteins, internalin (InlA) and InlB (3, 4). Although InlB is necessary and sufficient to promote entry into most cell types (5), internalin has a restricted tropism for cells expressing its specific receptor E-cadherin (6, 7). This cell-adhesion molecule allows cell sorting during development, adherens junction formation, and constitution of polarized epithelia (8). Latex beads coated with internalin or the noninvasive species *Listeria innocua* expressing internalin enter E-cadherin-expressing mammalian cells (6, 7). However, internalin interacts with a restricted number of E-cadherins, i.e., human, chicken, and guinea pig, but not with murine or rat E-cadherins (9).

E-cadherin is a transmembrane protein with an extracellular region composed of five repeat domains (ectodomain). The first two repeats mediate homophilic interaction. The intracytoplasmic domain interacts with proteins called catenins (10, 11). The 56-aa carboxyl-terminal part of E-cadherin cytoplasmic domain directly interacts with either β-catenin or γ-catenin (plakoglobin) (12), whereas its juxtamembrane (JM) domain interacts with p120-catenin (p120-ctn or p120-cas) (13–16). α-Catenin can bind to β-catenin and also interact with actin, thus providing a link between E-cadherin and the cytoskeleton (17, 18). Strong homophilic interaction, adherens junction formation, and cell compaction require connection of E-cadherin to actin via β- and α-catenins (10, 11, 19). The JM domain has been reported to play a role in E-cadherin clustering (13) and also in regulation of adhesion activity and suppression of cell motility (14–16, 20).

Inhibition experiments with cytochalasin D have shown that *L. monocytogenes*, like many other invasive pathogens, requires actin cytoskeleton rearrangements for entry into cells (21). It was thus of particular interest to study the role of the cytoplasmic domain of E-cadherin in the entry process. Our results clearly demonstrate that β- and α-catenins, which are recruited to the site of bacterial entry, are necessary for the dynamic events that induce the cytoskeleton rearrangements and plasma membrane extensions necessary for bacterial uptake.

Materials and Methods

Bacterial Strains, Cell Lines, Culture, Media, and Antibodies. *L. innocua* transformed with pRB474 (BUG 1528), *L. innocua* transformed with pRB474 harboring the *inlA* gene (BUG 1489), and *L. innocua* transformed with pP1B8 harboring an *inlB* construct (BUG 1642) have been described (7, 22). Caco-2 cells and LoVo cells were cultivated as described (6, 23). L2071 fibroblasts (ATCC CCL1.1) were cultivated in DMEM glutamax (GIBCO/BRL) supplemented with 10% FCS, and L2071-transfected cells were cultivated in the presence of 800 μg/ml of G418 (GIBCO/BRL).

Internalin and InlB were purified and coated onto far red fluorescent latex beads (Molecular Probes) as described (5–7, 24). HECD1 mouse monoclonal anti-human E-cadherin antibody was obtained from M. Takeichi, Kyoto University (25), anti-α-, β-, γ-, and p120-catenin antibodies were from Transduction Laboratories (Lexington, KY), and anti-β-actin was from Sigma. L7.7 mouse monoclonal anti-internalin and R695 rabbit polyclonal anti-vinculin antibodies have been described (26, 27).

DNA Constructs. Human E-cadherin (hEcad) cDNA (9) was subcloned at *Hin*dIII and *Xba*I sites in pcDNA3 (Invitrogen) and pSK− (Stratagene).

hEcadΔcyto lacks the entire hEcad cytoplasmic domain and harbors an additional valine in position 581. A PCR product obtained with OML36 (5′-GGCTTGGATTTTGAGGCCAAGC-3′) and OML37 (5′-TCCCCCCGGGCTACACTGCAGCTCTCCTCCGAAGAAACAGC-3′) using pSK−(hEcad) as a template was digested by *Kpn*I and *Sma*I and subcloned in pSK−, thus giving rise to pSK−(OML 36–37). The *Kpn*I and *Xba*I fragment from pSK−(OML 36–37) was subcloned in pcDNA3(hEcad), thus giving rise to pcDNA3(hEcadΔcyto).

hEcadΔCB, where CB is the β-catenin binding site, lacks the last 35 aa of hEcad cytoplasmic domain. hEcadΔCB cDNA was obtained from D. Rimm, Yale University, New Haven, CT and cloned at *Hin*dIII and *Xho*I sites in pcDNA3, thus giving rise to pcDNA3(hEcadΔCB).

hEcadΔJM harbors an internal deletion between amino acid positions 582 and 617 of hEcad. A PCR product obtained with OML42 (5′-AACTGCAGTGCACAGGGGCCTGGACGCTCGG-3′) and OML40 (5′-CAATTAACCCTCACTAAAGGG-3′) using pSK−(hEcad) as a template was digested by *Pst*I and *Xba*I and subcloned at these sites in pSK−(OML 36–37), thus giving rise to pSK−(OML 36–42). The *Kpn*I and *Xba*I fragment from pSK−(OML 36–42) was subcloned in pcDNA3(hEcad), thus giving rise to pcDNA3(hEcadΔJM).

Abbreviations: InlA, internalin; hEcad, human E-cadherin; JM, juxtamembrane; Cαctn, carboxyl-terminal 398 aa of mouse α-catenin; FACS, fluorescence-activated cell sorter; LB, lysis buffer; PR, proximal region; CB, β-catenin binding site; NT, nontransfected.

§To whom reprint requests should be addressed. E-mail: pcossart@pasteur.fr.

The publication costs of this article were defrayed in part by page charge payment. This article must therefore be hereby marked "*advertisement*" in accordance with 18 U.S.C. §1734 solely to indicate this fact.

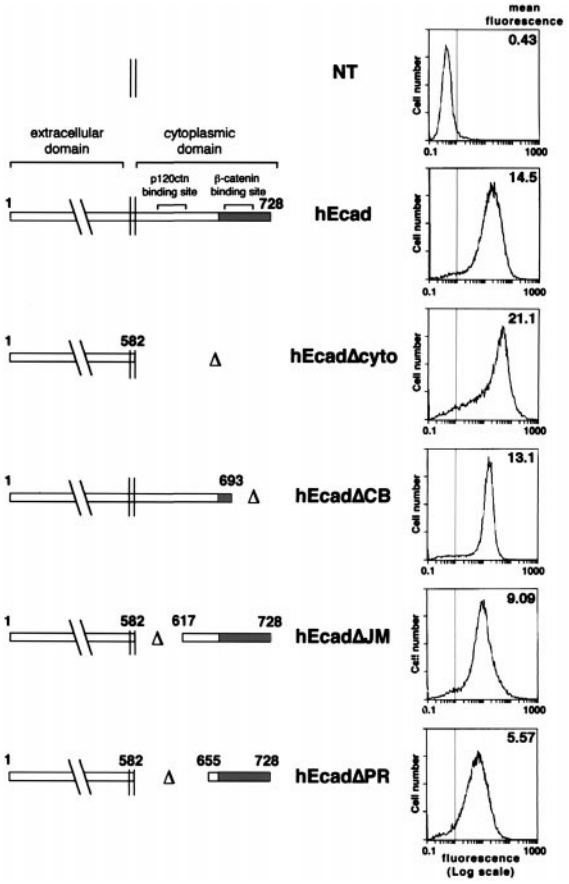

Fig. 1. Generation of stably transfected-cells expressing hEcad cytoplasmic variants. (*Left*) Schematic representation of hEcad and hEcad cytoplasmic variants. The double vertical bar represents the cytoplasmic membrane. Amino acids positions are indicated. (*Center*) Names of hEcad variants. (*Right*) FACS analysis of NT L2071 fibroblasts and stably transfected L2071 fibroblasts expressing hEcad or hEcad variants. Mean fluorescence after anti-hEcad and anti-mouse FITC-conjugated antibody labeling is indicated.

hEcadΔPR, where PR is the proximal region, harbors an internal deletion between amino acid positions 582 and 655 of hEcad. A PCR product obtained with OML39 (5′-AACTGCAGTGATTGATGAAAATCTGAAAGCGGC-3′) and OML40 (5′-CAATTAACCCTCACTAAAGGG-3′) using pSK−(hEcad) as a template was digested by *Pst*I and *Xba*I and subcloned at these sites in pSK−(OML 36–37), thus giving rise to pSK−(OML 36–39). The *Kpn*I and *Xba*I fragment from pSK−(OML 36–39) was subcloned in pcDNA3(hEcad), thus giving rise to pcDNA3(hEcadΔPR).

hEcad-Cαctn is a chimeric protein fusing hEcad transmembrane domain to the carboxyl-terminal 398 aa of mouse α-catenin (Cαctn). The *Cla*I and *Xba*I fragment encoding Cαctn was digested from pE1A3, a pSK−-derived plasmid provided by A. Nagafuchi (Kyoto University), harboring full-length mouse α-catenin cDNA (28). This restriction fragment was subcloned in pcDNA3(hEcad(1–581)-mEcad) (9). A *Kpn*I and *Cla*I restriction fragment from this plasmid was replaced by a PCR product obtained with oligonucleotides OML36 and OML45 (5′-CCATCGATAGCTCTCCTCCGAAGAAACAGC-3′) using pSK−(hEcad) as a template and digested with these two enzymes, thus giving rise to pcDNA3(hEcad-Cαctn). All PCR products were verified by sequencing.

Stable Transfections and Characterization of Transfected Cells. pcDNA3-derived plasmids were purified by using the Nucleobond AX kit (Macherey & Nagel), and transfections were carried out by using the calcium phosphate method. Transfected cells were selected in medium containing 800 μg/ml of G418 (GIBCO/BRL). Transfected L2071 cells expressing hEcad variants were dissociated in Hanks' medium containing calcium (GIBCO/BRL) and 0.1% trypsin (GIBCO/BRL), labeled with HECD1 mAb, and isolated by fluorescence-activated cell sorter (FACS) (Coulter). Four runs of FACS sortings allowed obtention of stably transfected cells. Surface expression level of hEcad variants was checked by FACS before each adhesion or invasion assay. It was stable and corresponded to the results presented in Fig. 1.

Transient Transfections and Quantification of Invasivity of Internalin-Coated Beads. Transient transfections and quantification of adhesion and invasivity of internalin-coated beads were performed as described (9). Level of entry of internalin-coated beads is expressed as a percentage and was calculated as the mean number (± SD) of intracellular beads divided by the number of total beads.

Cell Lysis, Immunoblotting, and Immunoprecipitation. Cells were lysed in lysis buffer (LB) {10 mM Tris·HCl, pH 7.5 containing 0.5% Triton X-100, 150 mM NaCl, 1 mM AEBSF [4-(2-aminoethyl)-benzenesulfonyl fluoride], 5 μg/ml each of chymostatin, antipain, pepstatin and leupeptin, and 0.2 mM sodium orthovanadate}. Cold LB was added to cells washed in PBS. Cells were rocked in the cold for 15 min, scraped, and centrifuged in a microfuge at maximum speed. For p120-catenin detection, 0.3% Triton X-100 was added to LB. Protein concentration was measured with the protein assay reagent (Bio-Rad). Supernatant was mixed with 2× SDS/PAGE sample buffer and heated, and equivalent amounts were run in 0.75-mm thick SDS/PAGE gels. Gels were transferred onto Immobilon-P membranes (Millipore) in a wet transfer apparatus for 2 h at 215 mA. Membranes were blocked in 5% milk-TBST (0.1% Tween 20-Tris-buffered saline) in the same buffer. All immunoblots used the anti-mouse IgG coupled with horseradish peroxidase. Immunoblots were developed with the ECL-Plus reagent (Amersham Pharmacia), and chemifluorescent emission was detected with a STORM (Molecular Dynamics) apparatus scanning with the blue laser, at voltage ranging from 650 V to 950 V.

For immunoprecipitation, 500 μg total protein as starting material and 1.5 μg of HECD1 were used, except for p120-catenin where 1,600 μg total protein and 3 μg of HECD1 were used. Lysates were precleared with Protein A Sepharose CL-4B (Amersham Pharmacia) for 1 h. After centrifugation, antibodies were added and lysates were mixed for 90 min. One hundred microliters of Protein A Sepharose CL-4B (Amersham Pharmacia; preswollen 30 mg/ml in LB) was added per 1 ml of lysate and mixed for 90 min. To precipitate mouse antibodies we added 2 μg rabbit anti-mouse IgG (Sigma) per tube. Immunoprecipitates were washed four times in LB, and the pellets were boiled in SDS/PAGE sample buffer to release bound material.

A monoclonal anti-β-actin antibody was used as a control for total protein in the lysate. Each blot was corevealed with this antibody and then quantified with the IMAGEQUANT program (Molecular Dynamics) to derive a ratio of the particular antigen to total actin to ensure that the results were representative in each case. For comparison cells also were lysed in a more dissociating RIPA buffer (0.15 mM NaCl/0.05 mM Tris·HCl, pH 7.2/1% Triton X-100/1% sodium deoxycholate/0.1% SDS). This treatment yielded a similar distribution of the antigens.

Cell Adhesion and Invasion Assays. Adhesion and invasion assays were performed immediately after FACS characterization of the cell lines. Cell adhesion tests (6) were performed with 1 μg of purified internalin or control BSA (Sigma) per well. Gentamicin survival assays (invasion tests) were performed by using *L.*

innocua transformed with the control plasmid pRB474 without insert or transformed with pRB474 harboring the *inlA* gene (7).

Detection of hEcad Clustering and Recruitment of Catenins and Actin at the Bacterial Entry Site. Cellular monolayers were seeded on 24-well plates (1×10^5 cells per well) 48 h before infection. Cells were washed twice with culture medium before bacterial inoculation and infected with a multiplicity of infection of 25 bacteria per cell in 500 μl of culture medium. Infection was performed at 37°C in 5% CO_2 for 45 min. Cells then were washed thrice with PBS solution, fixed-permeabilized with 3% paraformaldehyde, 0.5% Triton X-100 in PBS for 2 min, and postfixed with 3% paraformaldehyde in PBS for 20 min. Monolayers were washed with PBS, quenched with 0.5 M NH_4Cl in PBS during 10 min, and stained with the primary antibodies for 1 h. After washing with PBS, cells were stained with the secondary antibodies (Jackson ImmunoResearch) for 30 min. Finally, cells were washed with PBS, mounted in Mowiol, and analyzed in a Zeiss Axiovert 135 microscope.

Electron Microscopy. A total of 2×10^5 LoVo cells cultivated at 37°C in 10% CO_2 for 24 h in 2-cm diameter Petri dishes (Costar) were infected with 2×10^7 *L. innocua* expressing internalin diluted in DMEM. After 1 h of incubation at 37°C in 10% CO_2, cells were rinsed three times with DMEM and treated as described (29). Thin sections stained with uranyl acetate and lead citrate were examined on a Philips CM12 electron microscope operating at 80 KV (see Fig. 4 *R–T*).

Results

Generation of Stably Transfected Cells Expressing hEcad Cytoplasmic Variants. We generated a series of hEcad gene variants (Fig. 1) and transfected them into L2071 fibroblasts that do not express E-cadherin. Stably transfected cells were tested for adhesion to purified internalin and permissiveness to *L. innocua* expressing internalin.

Full-length hEcad is 728 aa long. hEcadΔcyto lacks the entire cytoplasmic domain. hEcadΔCB lacks the 35 carboxyl-terminal amino acids of the cytoplasmic domain. hEcadΔJM lacks the 35 first JM aa, and hEcadΔPR lacks the 73 proximal aa of the cytoplasmic domain (Fig. 1). Stable transfectants were selected by using G418 and several runs of FACS-sorting using HECD1, a monoclonal anti-hEcad antibody. For each cell line, mean fluorescence was measured by using the same arbitrary unit. It was almost similar for all variants (Fig. 1). It ranged from 5.57 for hEcadΔPR to 21.1 for hEcadΔcyto. Nontransfected (NT) L2071 cells had a mean fluorescence of 0.43. hEcadΔcyto-expressing cells exhibited a higher level of mean fluorescence, as previously reported for cell lines expressing a similar construct (10).

Expression of hEcad variants and α-, β-, γ-, and p120-catenins from total lysates was assessed by Western blotting and compared with that of NT cells or cells expressing hEcad. In agreement with previous reports, β-catenin expression was high in cells expressing hEcad variants with an intact CB, i.e., full-length hEcad, hEcadΔJM, and hEcadΔPR, with a calculated hEcad variant/β-catenin ratio around 1 (Fig. 2*A*). In cells expressing hEcadΔcyto or hEcadΔCB, β-catenin level was low and similar to that of NT cells, with a calculated hEcad variant/β-catenin ratio ranging from 13 to 33 (Fig. 2*A*). γ-Catenin was undetectable in NT and transfected cells, in line with other reports (30) (data not shown). α-Catenin expression was higher in cells expressing hEcad, hEcadΔJM, and hEcadΔPR and paralleled the pattern obtained with β-catenin. p120-Catenin expression was detected in all cell lines. Apparently none of the hEcad variants had any effect on its levels.

Catenin association with hEcad and hEcad variants was tested by coimmunoprecipitation. As shown in Fig. 2*B* and in agreement with previous reports (13, 14, 20), β- and α-catenins coimmunoprecipitated with hEcad (lane 1), hEcadΔJM (lane 4), and hEcadΔPR (lane 5), but not with hEcadΔcyto (lane 2) and hEcadΔCB (lane 3). Only hEcad exhibited detectable association with p120-catenin (lane 1), as shown in Fig. 2*B*. Despite optimization of the immunoprecipitation procedure (see *Materials and Methods*), association with p120-catenin could not be detected for hEcad cytoplasmic variants (Fig. 2*B*).

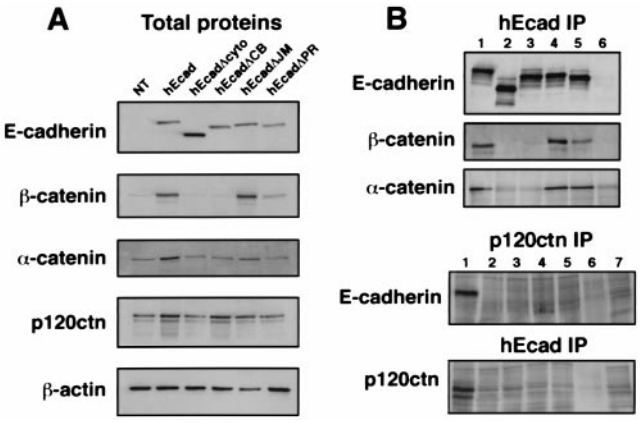

Fig. 2. Characterization of stably transfected-cells expressing hEcad cytoplasmic variants. (*A*) Expression of hEcad or hEcad variants, α-, β-, p120-catenins and β-actin in total cell lysates of stably transfected-cells (Western blot analysis). (*B*) Immunoprecipitations (IP) of hEcad or hEcad variants, α-, β-, and p120-catenins in stably transfected-cells. (*Top*) hEcad immunoprecipitations and revelation with anti-hEcad, anti-α-catenin, and anti-β-catenin antibodies. Lanes 1, hEcad; 2, hEcadΔcyto, 3, hEcadΔCB; 4, hEcadΔJM; 5, hEcadΔPR; and 6, NT. (*Middle*) p120-Catenin immunoprecipitations and revelation with anti-hEcad antibodies. Lanes 1–5 as in *Top*; lane 6, control without anti-p120-catenin antibody, and lane 7, control without cell lysate. (*Bottom*) hEcad immunoprecipitations and revelation with anti-p120-catenin antibodies. Lanes 1–5 as in *Top;* lane 6, control without anti-hEcad antibody, and lane 7, control without cell lysate.

The Ectodomain of E-Cadherin Is Sufficient for Internalin-Mediated Adhesion to Cells. Cell adhesion to immobilized internalin was tested. As shown in Fig. 3*A*, all transfected cells exhibited a significant and comparable level of adhesion to purified internalin in contrast to NT cells. These results indicate that the hEcad ectodomain is sufficient to mediate interaction with internalin and that the cytoplasmic domain plays no role in adhesion. In

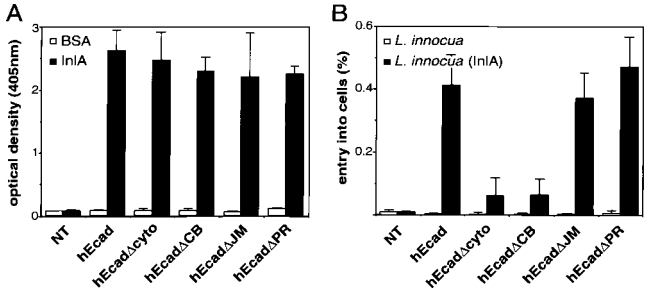

Fig. 3. Internalin-dependent adhesion to and entry into stably transfected-cells expressing hEcad cytoplasmic variants. (*A*) Cell adhesion to internalin of NT cells, hEcad and hEcad variants transfected cells. The optical density at 405 nm (hexosaminidase activity) linearly correlates with cell adhesion (BSA is used as a negative control, mean ± SD of four wells, see *Materials and Methods*). (*B*) Entry into NT cells, hEcad and hEcad variants transfected cells. Values are expressed as the percentage of bacteria resistant to gentamicin and are the mean ± SD of three independent assays.

agreement with these data, it was observed that internalin-coated beads or *L. innocua* expressing internalin adhere to cells expressing hEcad cytoplasmic variants as efficiently as to cells expressing full-length hEcad (data not shown). Similar data were obtained in cells expressing a liver cell adhesion molecule (chicken E-cadherin) variant lacking the entire cytoplasmic domain (data not shown).

The Cytoplasmic Domain of E-Cadherin Is Required for Internalin-Mediated Entry into Cells. Entry of *L. innocua* expressing internalin into the various hEcad variants-expressing cells was tested and quantified by using the gentamicin survival assay (21). As shown in Fig. 3*B* and in agreement with our previous results (7, 9), *L. innocua* expressing internalin did not enter into NT cells but invaded hEcad-transfected cells. Deletion of hEcad cytoplasmic domain dramatically impaired the level of entry, which was 6- to 7-fold lower in cells expressing hEcadΔcyto than in cells expressing hEcad. Similar results were obtained by using a double immunofluorescence labeling technique, allowing quantification of intracellular and extracellular bacteria or internalin-coated beads (data not shown). These data demonstrate that the hEcad cytoplasmic domain, although playing no role in the internalin-hEcad binding, is required for entry into cells.

The CB in E-Cadherin Is Critical for Internalin-Mediated Entry. To identify which part of hEcad cytoplasmic domain is required for entry of *L. innocua* expressing internalin into cells, we also used the gentamicin survival assay. As shown in Fig. 3*B*, hEcadΔJM- and hEcadΔPR-expressing cells allowed a level of entry comparable to that of hEcad-expressing cells, whereas in hEcadΔCB-expressing cells entry was 6- to 7-fold lower and was comparable to that in hEcadΔcyto-expressing cells. This result was confirmed by double immunofluorescence labeling using internalin-coated beads or *L. innocua* expressing internalin. Similar results were obtained in stably transfected cells expressing liver cell adhesion molecule (chicken E-cadherin) variants with similar deletions in the cytoplasmic domain (data not shown). Taken together, these results strongly suggest that the CB is the only region of the cytoplasmic domain necessary for entry.

An E-Cadherin/α-Catenin Fusion Protein Allows a Level of Internalin-Dependent Entry Comparable to that of Full-Length E-Cadherin. From the results obtained above, we reasoned that the CB is critical for entry because of its ability to connect hEcad to actin via β- and α-catenins. To address this issue, we generated a chimeric molecule (hEcad-Cαctn) linking directly the hEcad transmembrane domain to the carboxyl-terminal region of α-catenin, which has been shown to interact with actin (Cαctn) (31). Note that Cαctn does not encompass the vinculin nor the α-actin binding domains (32) (see Fig. 5, which is published as supplemental material on the PNAS web site, www.pnas.org). This construct, as well as full-length hEcad and hEcadΔCB cDNAs, were transiently transfected and expressed in L2071 fibroblasts, and the level of adhesion and entry of internalin-coated beads into these cells was measured. The level of adhesion was similar for the three constructs (data not shown). The hEcad-Cαctn fusion molecule allowed a level of entry (29.5% ± 3.2, mean ± SD) comparable to that of hEcad (31.0% ± 1.2) and five times higher than that of hEcadΔCB (6% ± 2.7). These results strongly suggest that the CB of E-cadherin is necessary for internalin-dependent entry because of its ability to link hEcad to the actin cytoskeleton.

Recruitment of E-Cadherin, β-Catenin, α-Catenin, p120-Catenin, and Actin During Internalin-Dependent Entry. We first studied whether hEcad clustered at the bacterial entry site. *L. innocua* bacteria expressing internalin induced hEcad clustering at their site of entry in Caco-2 cells (Fig. 4 *A* and *B*), the human enterocytic cell line in which internalin-dependent entry was originally described (3). This hEcad clustering was specifically induced by internalin, because control bacteria expressing no internalin and entering cells in an hEcad-independent manner, such as *L. innocua* expressing the InlB invasion protein, never induced hEcad clustering (Fig. 4 *A′–B′*). A similar result was obtained in LoVo cells (23), which allow, and at the same level, internalin- and InlB-dependent entry (unpublished results). In these cells, *L. innocua* expressing internalin but also internalin-coated beads induced hEcad clustering, whereas InlB-coated beads did not.

Because it is well established that the cytoplasmic domain of hEcad binds β-catenin, which in turn binds α-catenin, and p120-catenin, we examined by immunofluorescence whether these proteins were recruited at the entry site. We also investigated whether other components of the adherens junction were recruited. In addition to hEcad, β-, α-, and p120-catenins all were recruited at the entry site of *L. innocua* expressing internalin in Caco-2 cells (Fig. 4 *C* and *D*, *E* and *F,* and *G* and *H*, respectively) and LoVo cells, whereas vinculin and tensin were not (data not shown).

Because cytochalasin D, a drug inhibiting actin polymerization, abrogates entry of *Listeria* into cells (ref. 21 and unpublished results), we also examined whether F-actin accumulated at the entry site. It was indeed the case (Fig. 4 *Q*, *S*, and *T*). Moreover, hEcad, β-catenin, α-catenin, and actin colocalized at the entry site (Fig. 4 *I–Q*). After 15 or 30 min of infection, when hEcad clustering was already detectable at the site of entry, F-actin was hardly detectable (data not shown), suggesting that hEcad clustering precedes F-actin recruitment or polymerization. In all experiments, F-actin was indeed never observed in the absence of hEcad clustering. F-actin accumulation also was visualized by electron microscopy. It was not detectable during the attachment step (Fig. 4*R*), but was detectable at a later stage, when bacteria are being engulfed by the mammalian cell (Fig. 4 *S* and *T*). When cells were pretreated with cytochalasin D, F-actin was undetectable at the entry site. In those conditions hEcad clustering was still detectable underneath adherent bacteria (data not shown).

Taken together with the results described above, these observations suggest a critical role for E-cadherin cytoplasmic domain in entry, with hEcad mediating F-actin accumulation via β- and α-catenins.

Discussion

We have addressed the function of E-cadherin in internalin-mediated entry. We demonstrate here that in cells expressing E-cadherin, the ectodomain of this transmembrane protein mediates bacterial adhesion to mammalian cells and that the cytoplasmic domain is involved in and absolutely required for internalization. Moreover, the only region of the cytoplasmic domain required for entry is the carboxyl-terminal CB. A chimera consisting of the ectodomain of hEcad and the Cαctn, which interacts with actin, mediates entry as efficiently as full-length hEcad, revealing that for bacterial entry, the interaction with the cellular actin cytoskeleton is the important function of the E-cadherin–catenin complex. These results are in agreement with the observed coclustering of E-cadherin and β- and α-catenins at the site of entry. Moreover, the accumulation of F-actin at the site of entry after E-cadherin clustering demonstrates a dynamic participation of the E-cadherin complex in the F-actin recruitment and the cytoskeletal rearrangements that are necessary for entry.

The interaction between the first extracellular domain of E-cadherin and internalin was addressed elsewhere (9). This study revealed a very stringent specificity of interaction. Here we focused on the role of the cytoplasmic domain in *L. monocytogenes* adhesion and entry. Results clearly established that this domain is not involved in adhesion. Transfected cells expressing

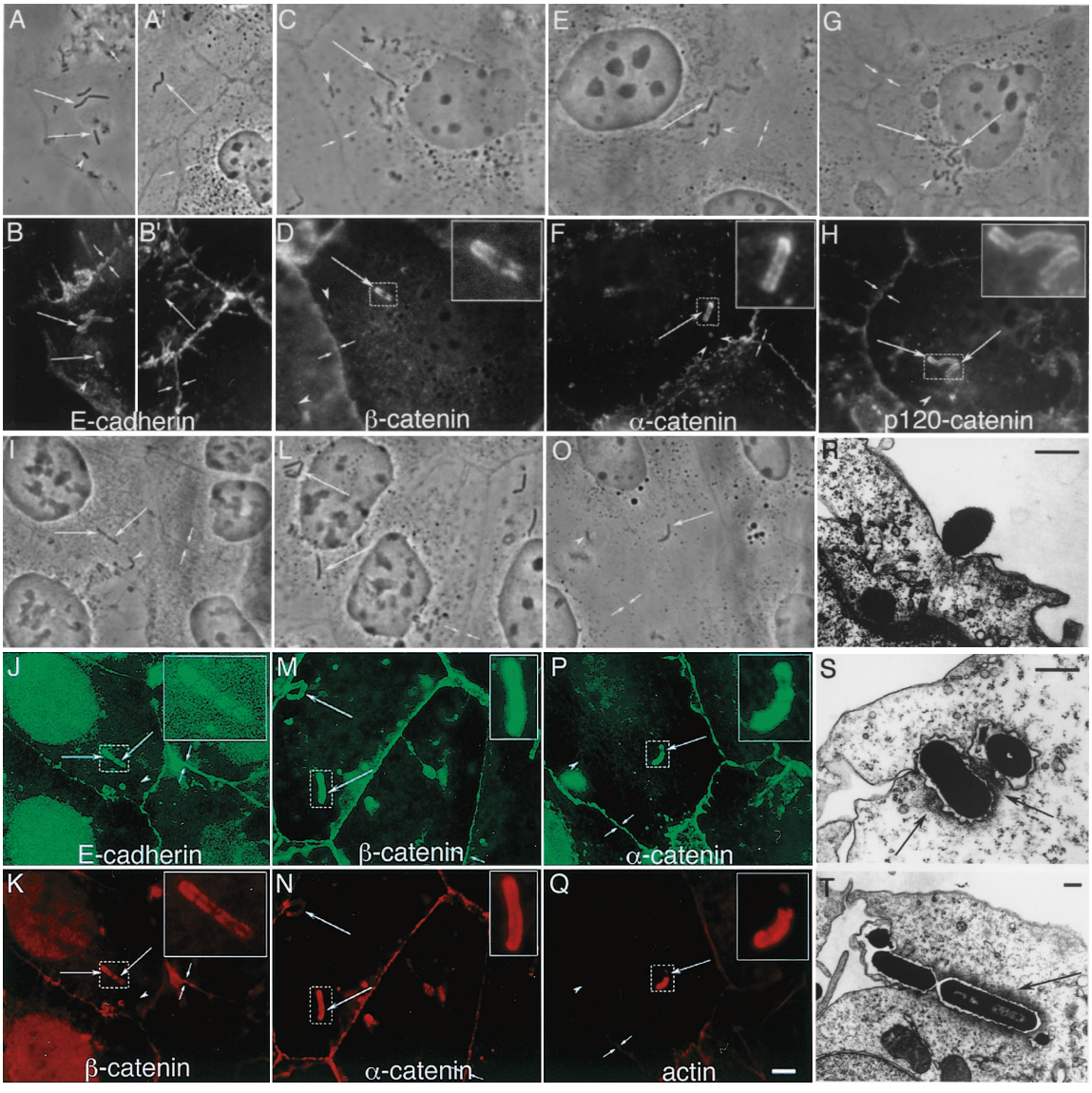

Fig. 4. Recruitment of hEcad, β-, α-, and p120-catenin and actin during entry of *L. innocua* expressing internalin into cells. (*A*–*Q*) Caco-2 cells infected with *L. innocua* expressing internalin. (*A*′ and *B*′) Caco-2 cells infected with *L. innocua* expressing InlB. (*R*–*T*) LoVo cells infected with *L. innocua* expressing internalin. (*A*, *A*′, *C*, *E*, *G*, *I*, *L*, and *O*) Phase contrast microscopy. (*B*, *B*′, *D*, *F*, *H*, *J*, *K*, *M*, *N*, *P*, and *Q*) Fluorescence microscopy. Arrows indicate sites where protein recruitment is observed around bacteria; arrowheads indicate sites where no protein recruitment is observed around bacteria, and small opposing arrows point to cell–cell junctions. (*Insets*) Magnification of the fluorescent labeling. (*A* and *B*) hEcad clustering during entry of *L. innocua* expressing internalin. (*A*′ and *B*′) Absence of hEcad clustering during entry of *L. innocua* expressing InlB. (*C* and *D*) β-catenin recruitment. (*E* and *F*) α-Catenin recruitment. (*G* and *H*) p120-Catenin recruitment. (*I*–*K*) hEcad and β-catenin colocalization. (*L*–*N*) β-Catenin and α-catenin colocalization. (*O*–*Q*) α-Catenin and actin colocalization. (Scale bar: 1 μm.) (*R*–*T*) Transmission electron micrographs showing actin recruitment (*S* and *T*, arrows) during *L. innocua* expressing internalin entry. (Scale bar: 500 nm.)

an hEcad variant lacking part or all of this domain interact with internalin as efficiently as cells expressing full-length hEcad. A similar result has been reported for the heterophilic interaction of E-cadherin with αE-β7 integrin (33). In contrast, homophilic interaction is strengthened by the cytoplasmic tail, and more precisely by the JM domain (13). These divergent results may reflect either technical differences or true differences between heterophilic and homophilic interactions, possibly because of differences in affinities.

Neither the JM region nor the PR of E-cadherin plays a role in the internalization process. The JM domain has been reported to suppress cell motility (20). The role of the larger PR, which spans the JM domain and mediates p120-catenin binding, is controversial. It has been reported to prevent E-cadherin dimerization and down-regulate adhesion (14, 15) or to induce cadherin lateral clustering and strengthen adhesion (13, 16). During bacterial entry, hEcad clustering and p120-catenin recruitment are observed at the entry site. Because all of the hEcad variants, even those lacking p120-catenin binding domain, also accumulated at the bacterial attachment site (see Fig. 6, which is published as supplemental material), this "clustering" appears as a bacterial-induced event, reflecting passive lateral cross-linking of the receptor, independent of p120-catenin. It is probable that this clustering/accumulation does not proceed as in the case of homophilic E-cadherin interactions. In particular, whether the oligomerization state of E-cadherin changes upon bacterial entry is unknown. It is thus possible that clustering of E-cadherin may favor a passive p120-catenin recruitment, reinforcing the hypothesis that p120 may not be critical for the morphological events that lead to entry but may still play another role in the cell during bacterial infection.

Deletion of the CB correlates with a 6- to 7-fold decrease in entry level. The precise location of the CB in the E-cadherin cytoplasmic domain remains a matter of debate. Although binding of β-catenin to this region is stronger when the whole cytoplasmic domain is present (34), the minimal CB is situated between amino acids 100 and 129 of the 150-aa long cytoplasmic tail (12) and deletion of the 35 last aa of the cytoplasmic tail totally abolishes β-catenin binding (ref. 11 and this work). Our findings that hEcadΔcyto and hEcadΔCB are the only deletions that dramatically impair internalin-mediated entry and that β-catenin is recruited at the entry site reinforce the hypothesis that the last 35 aa of E-cadherin are critical for β-catenin function and in the particular case of *Listeria* entry into cells.

A chimeric protein made of E-cadherin ectodomain and transmembrane domains fused to Cαctn is sufficient to create a link with the cytoskeleton and mediate intercellular adhesion as efficiently as wild-type E-cadherin (31). That transfected cells expressing a similar chimera allow bacterial entry as efficiently as cells expressing hEcad and that hEcad is clustered at the entry site and colocalize with β-catenin, α-catenin, and actin strongly suggests that the hEcad/β-catenin/α-catenin complex is acting by connecting internalin to the actin cytoskeleton. β-catenin thus plays the role of an adaptor protein in this process, and α-catenin is the key element in the actin cytoskeletal rearrangements. In agreement with these data, α-catenin negative human colon cancer cell variants (35) mediate a level of entry of *L. innocua* expressing internalin 10-fold lower than parental α-catenin positive cells (unpublished data). The importance of the catenin-mediated connection to the cytoskeleton also is supported by the electron microscopy observation that cytochalasin D treatment of hEcad-expressing cells has the same effect on entry than the deletion of the CB: i.e., in cytochalasin D-treated hEcad-expressing cells and hEcadΔCB-expressing cells, most bacteria (75%) appear extracellular (apposed to the cell plasma membrane and inducing no membrane deformation). In contrast, in untreated hEcad-expressing cells most bacteria (75%) are intracellular (unpublished data).

Many bacterial pathogens enter cells by a mechanism requiring remodeling of the actin cytoskeleton (36). *Listeria*, *Yersinia*, and *Neisseria* enter cells by the "zipper" mechanism during which plasma membrane is progressively apposed around the bacterial body (37). In these three examples, a ligand present on the surface of a particle (internalin for *Listeria*, invasin for *Yersinia*, opas for *Neisseria*,) interacts with a cell-adhesion molecule (E-cadherin, β1 integrins, and CD66, respectively). All these cell-adhesion molecules have an intracytoplasmic domain, allowing their connection to cytosolic partners and ultimately to the actin cytoskeleton. The present study, which demonstrates a critical role for the cytoplasmic domain of E-cadherin in *Listeria* entry, highlights that E-cadherin can drive actin cytoskeletal rearrangements. Interestingly, a very recent report has demonstrated that actin polymerization is the driving force for epithelial cell–cell adhesion (see Fig. 7, which is published as supplemental material) (38). This study has investigated the actin dynamics associated with intercellular adhesion and shows that intercellular junctions form by an active and dynamic process driven by actin filament polymerization. In that case, filopodia are formed that penetrate and embed into neighboring cells. That proteins such as vinculin are found in intercellular junctions and not detected in the bacteria-cell junctions suggest that although striking similarities are emerging, there may be significant differences most probably related to the different types of junctions that are formed. How different is the machinery that regulates the dynamics of this bacterial-induced phagocytosis from that underlying cell–cell adhesion deserves thorough investigation.

We thank H. Kiefer for help with the FACS analysis, D. Rimm for the gift of hEcadΔCB cDNA, A. Nagafuchi for the gift of mouse E α-catenin cDNA, W. Gallin for the gift of liver cell adhesion molecule constructs, M.M. Mareel for LoVo and α-catenin negative cells and helpful discussions, M. Takeichi for the gift of the HECD1 hybridoma cell line, P. Gounon for his help with the electron microscope, and L. Braun for the gift of InlB-coated beads. This work was supported by grants from Pasteur-Weizmann, BIOMED2 European Community, Délégation Générale pour l'Armement, Ministére de l'Education Nationale, de l'Enseignement Supérieur et de la Recherche, and Association pour la Recherche sur le Cancer. M.L. is a Ministére de l'Education Nationale, de l'Enséignement Supérieur et de la Recherche fellow, R.H. is a Human Frontier Science Program fellow, and J.P.-C. is an Association pour la Recherche sur le Cancer fellow. B.G. holds the E. Neter Chair in Cell and Tumor Biology.

1. Lorber, B. (1997) *Clin. Infect. Dis.* **24,** 1–11.
2. Cossart, P. & Lecuit, M. (1998) *EMBO J.* **17,** 3797–3806.
3. Gaillard, J.-L., Berche, P., Frehel, C., Gouin, E. & Cossart, P. (1991) *Cell* **65,** 1127–1141.
4. Dramsi, S., Biswas, I., Maguin, E., Braun, L., Mastroeni, P. & Cossart, P. (1995) *Mol. Microbiol.* **16,** 251–261.
5. Braun, L., Ohayon, H. & Cossart, P. (1998) *Mol. Microbiol.* **27,** 1077–1087.
6. Mengaud, J., Ohayon, H., Gounon, P., Mège, R. M. & Cossart, P. (1996) *Cell* **84,** 923–932.
7. Lecuit, M., Ohayon, H., Braun, L., Mengaud, J. & Cossart, P. (1997) *Infect. Immun.* **65,** 5309–5319.
8. Yap, A. S., Brieher, W. M. & Gumbiner, B. M. (1997) *Annu. Rev. Cell Dev. Biol.* **13,** 119–146.
9. Lecuit, M., Dramsi, S., Gottardi, C., Fredor-Chaiken, M., Gumbiner, B. & Cossart, P. (1999) *EMBO J.* **18,** 3956–3963.
10. Nagafuchi, A. & Takeichi, M. (1988) *EMBO J.* **7,** 3679–3684.
11. Ozawa, M., Ringwald, M. & Kemler, R. (1990) *Proc. Natl. Acad. Sci. USA* **87,** 4246–4250.
12. Stappert, J. & Kemler, R. (1994) *Cell Adhes. Commun.* **2,** 319–327.
13. Yap, A. S., Niessen, C. M. & Gumbiner, B. M. (1998) *J. Cell. Biol.* **141,** 779–789.
14. Ozawa, M. & Kemler, R. (1998) *J. Cell Biol.* **142,** 1605–1613.
15. Ohkubo, T. & Ozawa, M. (1999) *J. Biol. Chem.* **274,** 21409–21415.
16. Thoreson, M. A., Anastasiadis, P. Z., Daniel, J. M., Ireton, R. C., Wheelock, M. J., Johnson, K. R., Hummingbird, D. K. & Reynolds, A. B. (2000) *J. Cell Biol.* **148,** 189–202.
17. Aberle, H., Butz, S., Stappert, J., Weissig, H., Kemler, R. & Hoschuetzky, H. (1994) *J. Cell Sci.* **107,** 3655–3663.
18. Rimm, D. L., Koslov, E. R., Kebriaei, P., Cianci, C. D. & Morrow, J. S. (1995) *Proc. Natl. Acad. Sci. USA* **92,** 8813–8817.
19. Watabe, M., Nagafuchi, A., Tsukita, S. & Takeichi, M. (1994) *J. Cell Biol.* **127,** 247–256.
20. Chen, H., Paradies, N. E., Fedor-Chaiken, M. & Brackenbury, R. (1997) *J. Cell. Sci.* **110,** 345–356.
21. Gaillard, J. L., Berche, P., Mounier, J., Richard, S. & Sansonetti, P. J. (1987) *Infect. Immun.* **55,** 2822–2829.
22. Braun, L., Nato, F., Payrastre, B., Mazié, J.-C. & Cossart, P. (1999) *Mol. Microbiol.* **34,** 10–23.
23. Drewinko, B., Romsdahl, M., Yang, L., Ahearn, M. & Trujillo, J. (1976) *Cancer Res.* **36,** 467–475.
24. Braun, L., Dramsi, S., Dehoux, P., Bierne, H., Lindahl, G. & Cossart, P. (1997) *Mol. Microbiol.* **25,** 285–294.
25. Shimoyama, Y., Hirohashi, S., Hirano, S., Noguchi, M., Shimosato, Y., Takeichi, M. & Abe, O. (1989) *Cancer Res.* **49,** 2128–2133.
26. Mengaud, J., Lecuit, M., Lebrun, M., Nato, F., Mazié, J. C. & Cossart, P. (1996) *Infect. Immun.* **64,** 5430–5433.
27. Geiger, B. (1979) *Cell* **187,** 193–205.
28. Nagafuchi, A., Takeichi, M. & Tsukita, S. (1991) *Cell* **65,** 849–857.
29. Tilney, L. G. & Portnoy, D. A. (1989) *J. Cell Biol.* **109,** 1597–1608.
30. Papkoff, J. (1997) *J. Biol. Chem.* **272,** 4536–4543.
31. Nagafuchi, A., Ishihara, S. & Tsukita, S. (1994) *J. Cell Biol.* **127,** 235–245.
32. Imamura, Y., Itoh, M., Maeno, Y., Tsukita, S. & Nagafuchi, A. (1999) *J. Cell Biol.* **144,** 1311–1322.
33. Karecla, P. I., Green, S. J., Bowden, S. J., Coadwell, J. & Kilshaw, P. J. (1996) *J. Biol. Chem.* **271,** 30909–30915.
34. Chen, Y., Stewart, D. & Nelson, W. (1999) *J. Cell Biol.* **144,** 687–699.
35. Vermeulen, S. J., Bruyneel, E. A., Bracke, M. E., De Bruyne, G. K., Vennekens, K. M., Vleminckx, K. L., Berx, G. J., van Roy, F. M. & Mareel, M. M. (1995) *Cancer Res.* **55,** 4722–4728.
36. Dramsi, S. & Cossart, P. (1998) *Annu. Rev. Cell Dev. Biol.* **14,** 137–166.
37. Swanson, J. A. & Baer, S. C. (1995) *Trends Cell Biol.* **5,** 89–93.
38. Vasioukhin, V., Bauer, C., Yin, M. & Fuchs, E. (2000) *Cell* **100,** 209–219.